ISBN: 978-3-95450-231-8 ISSN: 2673-5490 doi: 10.18429/JACoW-IPAC2023-THPM018

OPTIMIZATION OF MECHANICAL ROBUSTNESS IN THE BOOSTER INJECTION BUMPERS

F. Lackner*, M. Atanasov, B. Balhan, C. Baud, J. Borburgh, M. Walraven**
CERN, European Organization for Nuclear Research, [CH-1211] Geneva, Switzerland
**University of Applied Sciences Alkmaar, [1817MN] Alkmaar, The Netherlands

Abstract

During the Long Shutdown 2 (LS2) at CERN, the new Linac4 (L4) accelerator has been successfully connected to the PS Booster (PSB) to inject 160 MeV beam into the 4 superposed PSB rings. The horizontal displacement of the circulating beam during injection relies on 4 pulsed dipole magnets. During the initial run of the new magnet system, non-conformities have been observed. These could be traced back mainly to early fatigue effects, some of which were in brazed joints on the coil cooling circuit. An extensive program has been launched to improve the brazing technology for the spare coil manufacturing. This effort has been combined with numerical computations as well as destructive and non-destructive testing of brazed joints, allowing to identify critical stress domains resulting in fatigue sensitive areas. This paper describes the applied methodology and implements measures to increase the robustness of the magnet coils. The achieved improvements have been validated by testing based on an instrumented coil, allowing to correlate stress-strain measurements with results from the structural and transient numerical computation.

INTRODUCTION

The BSW coils have been manufactured from oxygen free electronic grade hollow copper conductor. A manual bending process is used to form the coil shape. The coil geometry of the septum magnet BSW1 consists of a single layer coil, the injection bumpers BSW2-4 use a double layer coil. As the magnets are exposed to 10 million current pulses per year, the challenging operational conditions require a robust mechanical design in order to maximize their life cycle. Preventive maintenance and inspection plans have been implemented to to track any sign of early degradation. The initiated manufacturing optimization process will allow to further increase the operational life cycle while reducing the amount of major non-conformities. Figure 2 shows an overview of the coil and coil to half yoke assembly, and Table 1 provides the magnet main parameters. Details about the design and operating conditions are described in [1], [2].

The BSW1-4 coils consist of:

- A water-cooled oxygen free conductor with a square cross-section of 5 mm. The conductor is manually bend into the coil shape, flame brazed copper reinforcements on the coil longitudinal direction increase the magnetic performance, and act as mechanical reinforcement.

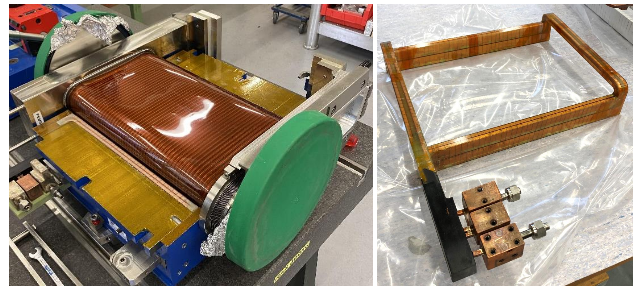

Figure 1: Left: Photograph of a BSW half yoke with view on the vacuum chamber. Right: BSW2-4 coil incl. cooling circuit connector (water blocks).

- A flame brazed water block made from copper for the cooling circuit connection.
- Coil insulation which consist of a manually wrapped 50% overlapping S2 fiber-matrix of 0.2 mm, vacuum impregnated using CDT101 resin. The achieved final insulation thickness is 1 mm. During the coil-yoke assembly, a 0.1 mm thick polyimide insulation layer is applied in the yoke to coil interface.
- The half yokes are assembled using bolted connections. Mechanical stoppers are implemented to provide repetitive assembly conditions, avoiding over constraining the coil.

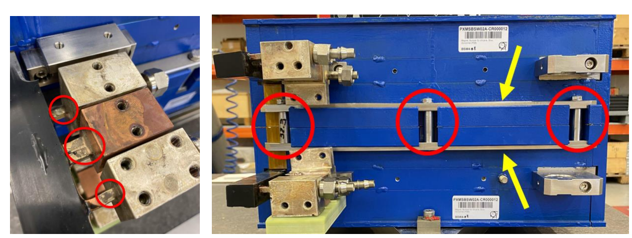

Figure 2: Left: Water block flame brazed joints. Right: Yoke side view with mechanical assembly stoppers and load distribution bars (yellow arrow).

NON-CONFORMITIES & ROOT CAUSE INVESTIGATIONS

Several non-conformities observed throughout the initial operation period triggered a root cause analysis. The non-conformities mainly relate to early fatigue failure modes due to the high amount of operation cycles. These failures require stopping the accelerator operation and result usually

* Friedrich.Lackner@cern.ch

ISBN: 978-3-95450-231-8 ISSN: 2673-5490 doi: 10.18429/JACoW-IPAC2023-THPM018

Table 1: BSW Magnet Parameters (March 2023)

Parameter	Unit	BSW1 / BSW2-4
Integral field	mT/m	126.3 / 126.4
RMS current	A	457 / 220
Electric peak current	A	6868 / 3298
Repetition time (Total cycle)	s	0.9
Flat top duration	ms	1
Conductor height x width	mm	5 x 5
Cooling channel diameter	mm	3
Coil length, width	mm	332.8 / 347.8
Coil length, width	mm	201 / 268
Cooling water pressure	bar	12
Flow rate	L/min	2.5 / 1.5

in a magnet exchange. The following observations have been made during the analysis, triggering the indicated actions:

- Water leaks and signs of initial galvanic corrosion in brazed joints of coil-to-water block connections. A visual and microscopic inspection of brazed areas, as well as chemical analysis of the corrosion residuals, have been launched.
- Micro-cracks in the conductor bending regions. Static structural and transient Finite Element Analysis (FEA) have been carried out to identify critical stress regions and their impact on early mechanical fatigue. In parallel, applied assembly conditions and coil pre-stress have been studied.
- Areas of weak mechanical stability in the brazing joints have been identified. A research for potential alternative technologies, brazing alloys as well as flux materials was launched. In order to qualify the brazed joints, a large amount of sample tests have been performed. Alternative materials have been qualified according to their shear stress limitations and based on computed tomography. The entire brazing procedure and quality control process have been reviewed, available standards in brazing technology have been consulted [3], [4].

Brazing Procedure & Process Qualification

A new brazing procedure has been defined based on recommendation from the ISO standards. This mainly concerns the distribution of individual roles for the brazing preparation, the process of brazing, and the subsequent quality control. In parallel, brazing sample tests have been launched [3]. In order to further reduce the risk for galvanic corrosion, silver-copper-phosphorus brazing filler metals (SIL-FOS) have been extensively tested as an alternative for brazing the copper-copper joints. This will avoid using the previously applied halogen (fluoride) based corrosive flux.

Shear test samples have been produced following all recommendations given by ISO 17779:2021. Two grades of the above-mentioned brazing filler material have been compared, differing in the silver content (5% and 15%). The sample,

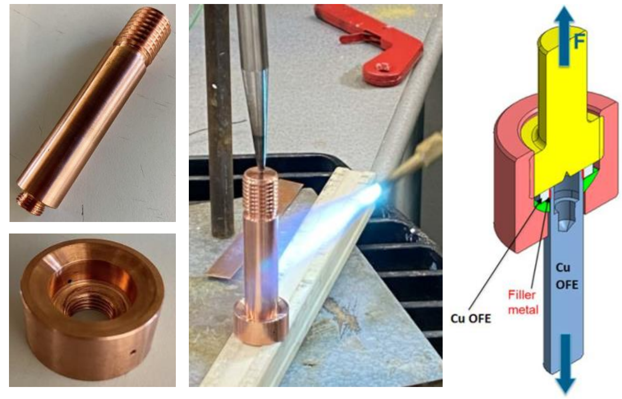

Figure 3: Left: Shear sample, diameter:16 mm, Center: brazing precess, Right: Tensile test of shear sample

brazing process and shear test concept is shown in Fig. 3. Probe and probe-head assembly allow for a predefined brazing gap and degassing via lateral capillaries. Temperature gauges have been used to achieve repetitive brazing conditions, Seven high quality shear samples have been prepared and qualified by computed tomographic inspection. The test samples have been tested on the ZwickRoell electromechancial testing machine (Z250). HeBoCoat has been applied on the contact interface prior performing the test. The samples brazed with SIL-FOS with the 15% Ag content had the highest shear strength and gave the most repetitive results (based on the standard deviation).

Table 2: Results from the Shear Tests of SIL-FOS

Alloy	Shear strength MPa	Stand. dev.
SIL-FOS 5	119.4	21.3
SIL-FOS 15	140.8	2.9

FEA Studies on Coil Stress and Assembly Pre-load

The BSW coils require to withstand the Lorentz force, enerated by the magnetic field, every 1.2 seconds with a peak current plateau of 0.2 ms. The resulting longitudinal and transversal forces are summarised in Table 3

Table 3: Electromagnetic Forces on Long and Short Coil Site

Parameter	Unit	Value
Long site	kN	1.9
Short site	kN	1.83

FEA computations have been conducted under static structural application of Lorentz forces on the coil. The assumption of coil rebounding after current excitation is assumed, applying an inverse nominal load condition. This approach allows to verify the worst case stress-strain conditions. A transient FEA has allowed to validate this coil dynamic movement throughout the short excitation cycle and confirmed an

ISBN: 978-3-95450-231-8 ISSN: 2673-5490 doi: 10.18429/JACoW-IPAC2023-THPM018

80% rebound effect after excitation. The results under static load indicate a maximum equivalent stress in the small coil bending radius of 130 MPa. A crack has been observed after a coil non-conformity and microscopic inspection, see also Fig. 4. In order to reduce these local peak stresses, reinforcement bars made from G11 glass epoxy laminate have been implemented in order to reduce the induced bending strain. The FEA verification has shown that the reinforcement significantly reduces the peak stress to 20 MPa, as shown in Fig. 5. The imbalance in the stress on the coil extremities can be explained by the additional rigidity given by the water block to coil fixation. The brazed joint areas indicate equivalent stresses of up to 14 MPa.

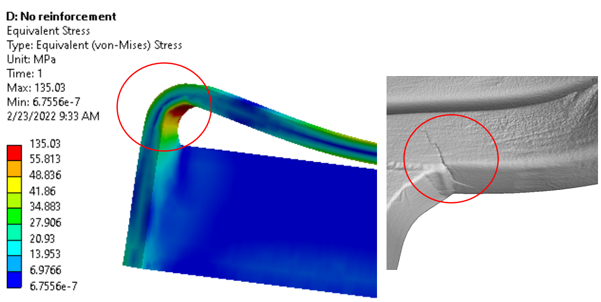

Figure 4: Left: Equivalent critical stress due to Lorentz force, Right: Observed crack after non-conformity inspection

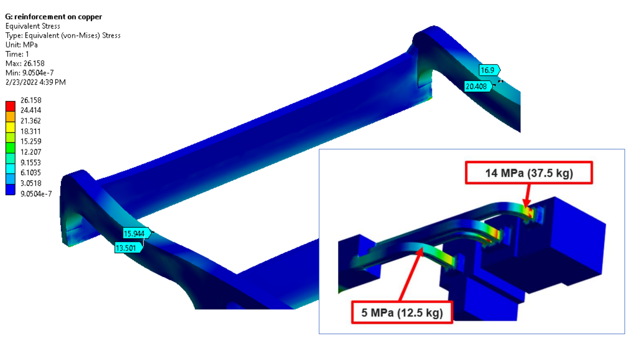

Figure 5: Left: Reinforced copper coil, Right: Critical stress in water block brazing joint regions

Impact of Vertical Pre-load on Bending Stress

The transient model has also underlined that any coil movement is strongly dependent on the applied assembly pre-load. Yoke and coil mid-plane assembly tolerances have therefore been verified using pressure sensitive film from Fuji [5]. This has allowed to achieve a uniform contact condition in the yoke and coil mid-plane. The contact in the coil mid-plane (Fig. 6) has been achieved by adding a 0.15 mm thick polyimide layer, slightly increasing the vertical assembly coil-yoke and coil-coil contact stiffness. The stress values have been verified using an available Matlab script, indicated a low average contact stress of 17 MPa in the mid-planes. The pressure distribution and shimming location are shown in Fig. 6. The pressure distribution on the mid-plane corresponds to (A) for the yoke and (B) for the coil [6].

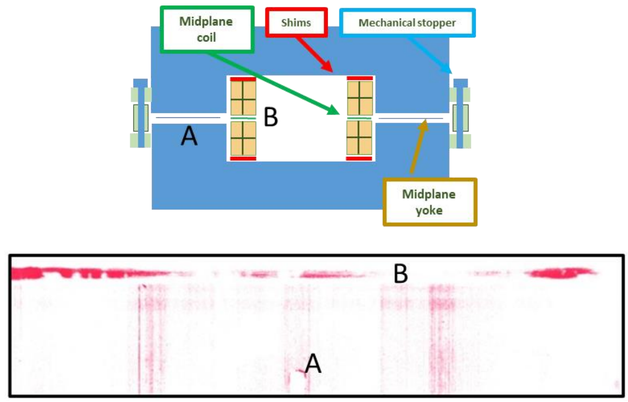

Figure 6: Top: Shimming and mid-plane location, Bottom: Pressure distribution on coil and yoke mid-plane (Fuji prescale film)

A BSW4 coil has been electrically instrumented by 7 strain gauges and tested on the test bench with 10^5 nominal current pulses. The analysis of the measurements is currently ongoing, indicating an effective 7% reduction of the dynamic strain amplitudes under the small shimming. Prior to increasing the load conditions, a careful visual inspection of the interface planes will be carried out. It is important to avoid plastic deformation or risk for crack initiation in the fiber-resin matrix, due to high pre-load conditions.

CONCLUSION

An optimization of the mechanical robustness of the booster injection bumpers has been launched. Non-conformities required to improve the robustness of flame brazed joints and to minimize the Lorentz force induced mechanical stress. A stringent change in the brazing procedure has been implemented according recommendations from the international standards. Signs of galvanic corrosion in the brazing joints required to qualify a non-flux based brazing process. SIL-FOS 15 has been successfully qualified, based on shear tests, now used for the production of BSW spare coils. An FEA campaign has underlined the importance of adding reinforcements on the coil short sides, reducing critical bending stress by a factor 5. Vertical coil shimming and strain gauge instrumented coil tests have underlined the importance of further decreasing the bending strain based on uniform vertical pre-constraints. The currently ongoing coil fabrication is carried out based on the described latest findings and will further increase the robustness and operation time of the magnets.

ISBN: 978-3-95450-231-8 ISSN: 2673-5490 doi: 10.18429/JACoW-IPAC2023-THPM018

REFERENCES

[1] W. J. M. Weterings, C. Bracco, L. O. Jorat, M. Meddahi, R. Noulibos, and P. Van Trappen, “The New Injection Region of the CERN PS Booster”, in *Proc. 10th Int. Particle Accelerator Conf. (IPAC’19)*, Melbourne, Australia, May 2019, pp. 2414–2417. doi:10.18429/JACoW-IPAC2019-WEPMP039

[2] E. Benedetto, B. Balhan, J. Borburgh, C. Carli, V. Forte, and M. Martini, “Detailed Magnetic Model Simulations of the H-Injection Chicane Magnets for the CERN PS Booster Upgrade, including Eddy Currents, and Influence on Beam Dynamics”, in *Proc. 5th Int. Particle Accelerator Conf. (IPAC’14)*, Dresden, Germany, Jun. 2014, pp. 1618–1620. doi:10.18429/JACoW-IPAC2014-TUPRI027

[3] D. P. Sekulic, Advances in brazing, science technology and applications, 2013. ISBN: 978-1-84569-532-3

[4] M. Schwartz, Brazing, second edition, 2003. ISBN: 978-0-87170-784-0

[5] Product Information FujiFilm Pressure Measurement Film, http://www.fujifilm.com/products/prescale/prescalefilm

[6] M. Walraven, Characterization of critical design parameters in the BSW4 coils., 2023, CERN report. EDMS 2816557